

# Structure Function Results from ZEUS

A. Kappes<sup>a</sup> for the ZEUS Collaboration

<sup>a</sup>Physikalisches Institut der Universität Bonn, Nußallee 12, D-53115 Bonn

This contribution presents recent ZEUS results on proton structure functions at HERA. The inclusive  $\phi(1020)$ -meson cross section was measured, and it was used to determine the  $s$ -quark content of the proton. The structure function  $F_2$  was extracted using initial-state radiative events. Neutral and charged current cross sections were used to extract the structure function  $xF_3$  and measure the mass of the  $W$  boson, respectively. A NLO QCD fit to ZEUS data and fixed target cross sections was employed to determine the parton density functions of the quarks and of the gluon inside the proton.

## 1. Deep inelastic $ep$ scattering (DIS)

The Hadron-Elektron-Ringanlage HERA at DESY in Hamburg accelerates electrons/positrons and protons to energies of  $E_e = 27.5$  GeV and  $E_p = 920$  GeV (900 GeV before 1998), yielding a center-of-mass energy,  $\sqrt{s}$ , of 318 GeV (300 GeV before 1998). In DIS events the interaction between the two particles can either occur via a neutral (NC,  $\gamma$  or  $Z$ ) or a charged current (CC,  $W$ ) process. The reaction can be described by two of the three variables  $Q^2$ ,  $x$ -Bjorken and  $y$ . Here,  $Q^2$  is the negative of the squared 4-momentum transfer between lepton and proton and  $y$  is the inelasticity.

The NC cross section can be written as

$$\frac{d^2\sigma(e^\pm p)}{dx dQ^2} = \frac{2\pi\alpha^2}{x Q^4} [Y_+ F_2^{\text{NC}} \mp Y_- x F_3^{\text{NC}} - y^2 F_L^{\text{NC}}]$$

$$(F_2^{\text{NC}}, xF_3^{\text{NC}}) = x \sum_{q=u\dots b} (A_f, B_f) [(q + \bar{q}, q - \bar{q})],$$

where  $q$  and  $\bar{q}$  are the parton density functions (PDFs) of quarks and antiquarks and  $Y_\pm = 1 \pm (1 - y)^2$ .  $A_f$  and  $B_f$  depend on  $Q^2$  only and contain the vector and axial-vector couplings as well as the propagator terms. The reduced cross section is defined as  $\tilde{\sigma}^{\text{NC}} = \frac{d^2\sigma^{\text{NC}}}{dx dQ^2} \times \frac{x Q^4}{2\pi\alpha^2 Y_+}$ .

The CC cross section is similar to that of NC

$$\frac{d^2\sigma(e^- p)}{dx dQ^2} = \frac{G_F^2}{4\pi x} \frac{M_W^4}{(Q^2 + M_W^2)^2} \times [Y_+ F_2^{\text{CC}} + Y_- x F_3^{\text{CC}} - y^2 F_L^{\text{CC}}]$$

$$(F_2^{\text{CC}}, xF_3^{\text{CC}}) = x [(u + c + \bar{d} + \bar{s}, u + c - \bar{d} - \bar{s})],$$

however, for electrons the  $W$  couples only to positively charged quarks. The reduced cross section is defined as  $\tilde{\sigma}^{\text{CC}} = \frac{d^2\sigma^{\text{CC}}}{dx dQ^2} \times \frac{4\pi x}{G_F^2} \frac{(Q^2 + M_W^2)^2}{M_W^4}$ .

## 2. Inclusive $\phi(1020)$ -meson production

$\phi$  mesons in DIS can be either formed directly from  $s$  quarks inside the proton or indirectly from  $s$  quarks produced via BGF or in the hadronization process. Generally, the cross section for indirect production is much larger than that for the direct one, rendering the measurement of the  $s$ -quark content of the proton rather difficult. However, for direct  $\phi$  production the variable  $x_p(\phi) = 2p(\phi)/Q$  clusters around 1, where  $p(\phi)$  is the  $\phi$  momentum in the Breit frame. Therefore, at high  $x_p(\phi)$  inclusive  $\phi$  production is sensitive to the  $s$ -quark content of the proton.

The  $e^+p$  data set used was recorded during the run periods 1995–97 at a center of mass energy of 300 GeV and corresponds to an integrated luminosity of  $\mathcal{L} = 45.0$  pb<sup>-1</sup>. The cross section was measured in the range  $10 < Q^2 < 100$  GeV<sup>2</sup> and  $2 \times 10^{-4} < x < 10^{-2}$ . The preliminary cross section is  $\sigma(e^+p \rightarrow e^+\phi p) = 0.506 \pm 0.022$  nb [1]. In Fig. 1 for  $x_p \lesssim 0.8$ , where the indirect contribution to  $\phi$  production is expected to dominate and theoretical predictions are somewhat uncertain, large differences between the various models can be observed. However, for  $x_p > 0.8$  the differ-

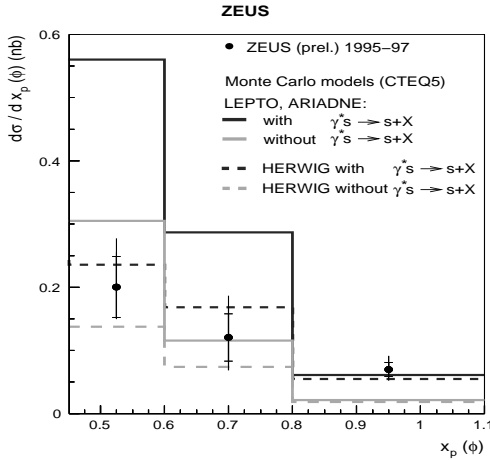


Figure 1.  $d\sigma/dx_p$  as a function of  $x_p$ . The dark (light) lines correspond to predictions using LEPTO/ARIADNE and HERWIG with (without) inclusion of an  $s$ -quark content of the proton.

ences among models with  $s$ -quark content on the one hand and among those without  $s$ -quark content on the other hand are small compared to the measurement error. Here, models featuring an  $s$ -quark content of the proton are clearly required by the data.

### 3. $F_2$ from initial-state radiative events

The acceptance of the ZEUS main detector for scattered electrons is limited towards small scattering angles to  $\theta^* \gtrsim 4^\circ$  ( $Q^2 \gtrsim 2 \text{ GeV}^2$ ). One possibility to measure  $F_2$  at even lower  $Q^2$  values is to use initial-state radiative (ISR) events where a photon was radiated from the incoming lepton. Due to the energy carried by the photon,  $E_\gamma$ ,  $\sqrt{s}$  of the reaction is reduced by a factor  $(E_e - E_\gamma)/E_e$ . As a consequence, electrons with low  $Q^2$  are scattered into the main detector.

The  $F_2$  measurement [2] was performed on a small fraction of the 1996  $e^+p$  data set ( $\mathcal{L} = 3.8 \text{ pb}^{-1}$ ). It covers the range  $0.3 < Q^2 < 22 \text{ GeV}^2$ ,  $1 \times 10^{-5} < x < 3 \times 10^{-2}$  and fills the gap in the  $F_2$  coverage of the kinematic plane around  $1 \text{ GeV}^2$  and  $x > 3 \times 10^{-4}$ . Fig. 2 shows that the ISR  $F_2$  values agree well with other measurements both in the lower and upper  $Q^2$  region. Theoretical predictions based on the ZEUS NLO-QCD

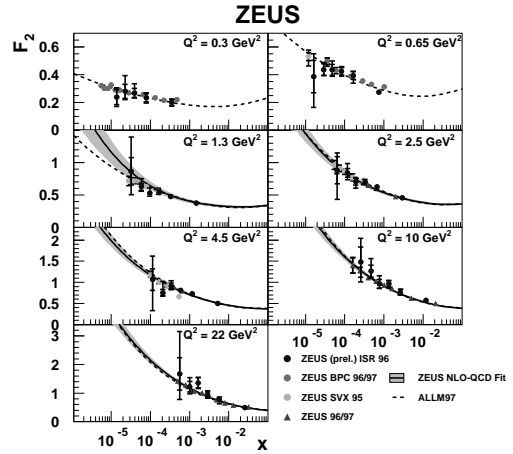


Figure 2.  $F_2$  as a function of  $x$  in different  $Q^2$  bins. In addition to the ISR data also former measurements are shown together with theoretical predictions.

fit are in good agreement with the ISR data for  $Q^2 > 2.5 \text{ GeV}^2$ . For lower  $Q^2$  a Regge inspired fit (ALLM97) yields a good description of the data. ISR events will allow a direct measurements of  $F_L$  in the future.

### 4. High- $Q^2$ NC cross sections from $e^-p$ DIS

Electromagnetic interactions are invariant under  $P$  and  $C$  transformations and hence,  $\sigma^{\text{NC}}(e^-p) \approx \sigma^{\text{NC}}(e^+p)$  for  $Q^2 \ll M_Z^2$  ( $\gamma$ -only exchange), where  $M_Z$  is the mass of the  $Z$  boson. However, weak interactions do not preserve  $P$  and  $C$  but only approximately  $CP$ . As a consequence  $\sigma^{\text{NC}}(e^-p) > \sigma^{\text{NC}}(e^+p)$  for  $Q^2 \gtrsim M_Z^2$ , where in addition to the  $\gamma$  exchange also the  $Z$  exchange gives a considerable contribution to the cross section. The parity violating terms of  $\sigma^{\text{NC}}(e^\pm p)$  are combined in the structure function  $x F_3$ , whereas those in  $F_2$  are invariant under  $P$ . A comparison of  $e^-p$  and  $e^+p$  cross sections yields a direct test of the electroweak sector of the Standard Model.

The  $e^-p$  data set used was recorded in 1998–99 ( $\mathcal{L} = 15.9 \text{ pb}^{-1}$ ). The NC cross sections were measured in the range  $185 < Q^2 < 50\,000 \text{ GeV}^2$  and  $0.0037 < x < 0.75$  [3]. Figure 3 shows good agreement between the theory computed with the ZEUS fit to the 1996–97 data (ZEUS-S) and the

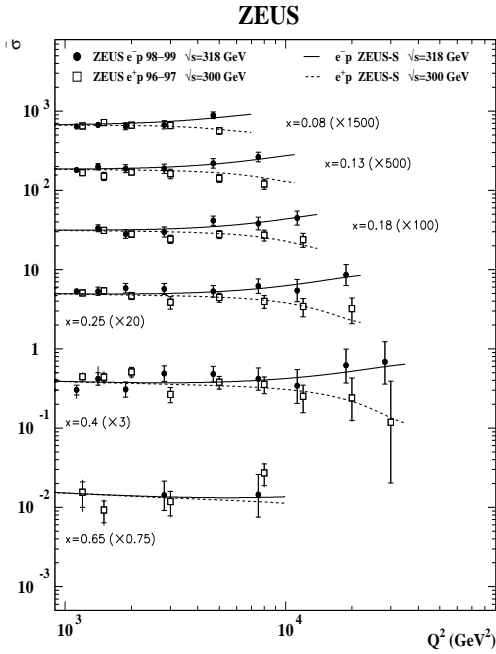


Figure 3. The reduced cross section  $\tilde{\sigma}$  as a function of  $Q^2$  in different  $x$  bins.

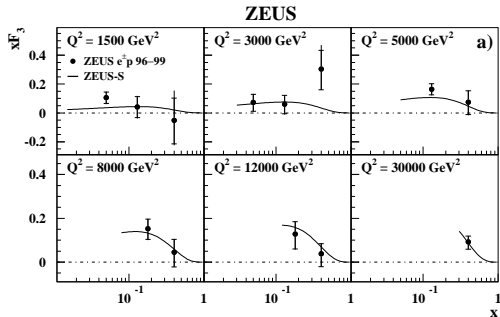


Figure 4.  $xF_3$  as a function of  $x$  in  $Q^2$  bins.

data, where only points with  $Q^2 > 1000 \text{ GeV}^2$  are shown. Also plotted is the  $e^+p$  measurement from 1996–97 data based on  $30 \text{ pb}^{-1}$ . A comparison of  $e^-p$  and  $e^+p$  cross sections shows an increase of the former and a decrease of the latter as expected from the  $Z$  exchange. The structure function  $xF_3$  extracted from these data is shown in Fig. 4 and is compared to the prediction from the ZEUS-S NLO fit. The measurement yields  $xF_3 \neq 0$  and the data is well described by the theory using ZEUS-S. The large errors of the measurement are

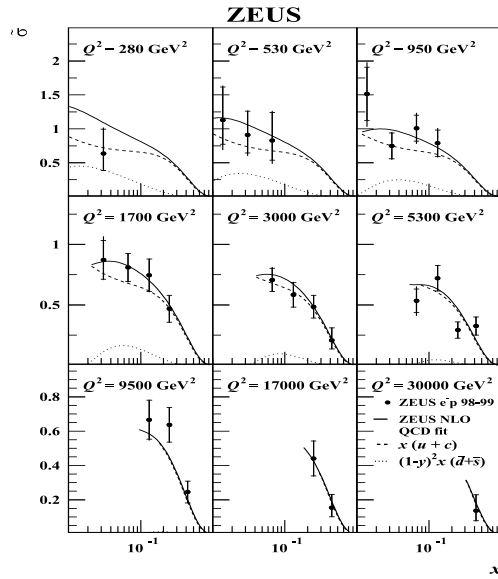


Figure 5. Reduced charged current cross section as a function of  $x$  in different  $Q^2$  bins. Shown are the measured and expected cross sections and the contributions from  $u + c$  and  $\bar{d} + \bar{s}$  quarks.

dominated by the low  $e^-p$  statistics.

## 5. High- $Q^2$ CC cross sections from $e^-p$ DIS

In contrast to NC reactions CC reactions are purely weak and exhibit therefore a more direct dependence on the weak parameters. Also, due to the charge-selective coupling of the  $W$  boson, measuring CC cross sections yields information about the flavor content of the proton.

The  $e^-p$  data set used for the measurement [4] was recorded in 1998–99 ( $\mathcal{L} = 16.4 \text{ pb}^{-1}$ ). The measurement was performed for  $280 < Q^2 < 30000 \text{ GeV}^2$  and  $0.015 < x < 0.42$ . Figure 5 shows good agreement between data and predictions using ZEUS-S. At high  $x$  the cross section is dominated by the  $u$  (valence) quarks and a measurement in this region allows a direct determination of the  $u$  quark PDF of the proton. At low  $x$  the contribution from the  $(\bar{d} + \bar{s})$  sea is also small due to the helicity structure of the reaction. As the CC cross section directly depends on the mass of the  $W$  boson,  $M_W$ , a fit of  $M_W$  to  $d\sigma/dQ^2 \propto M_W^4 / (Q^2 + M_W^2)^2$  was per-

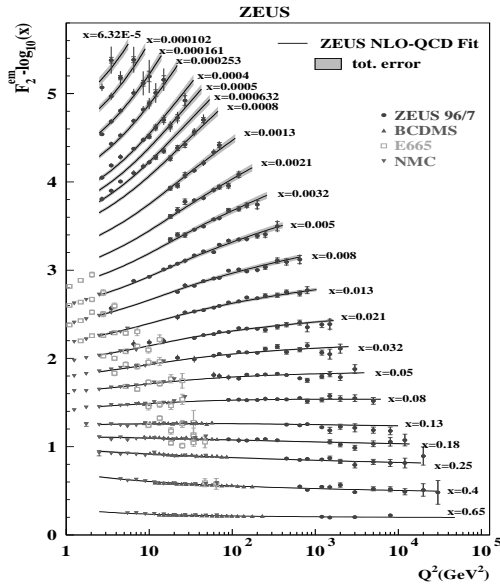


Figure 6.  $F_2$  as a function of  $Q^2$  in bins of  $x$ .

formed. The fit yielded  $M_W = 80.3 \pm 2.1$  (stat)  $\pm 1.2$  (sys)  $\pm 1$  (PDF) GeV. A comparison with the fit to the  $e^+p$  data ( $M_W = 81.4^{+2.7+2.0+3.3}_{-2.6-2.0-3.0}$  GeV) shows good agreement within errors. The systematic and PDF uncertainties are much smaller for the more recent measurement. In case of the systematic uncertainty, this is due to a much improved understanding of the energy scale uncertainty. On the other hand, the  $u$ -quark PDF, dominating the  $e^-p$  cross section, is much better known than the  $d$ -quark PDF which mainly determines the  $e^+p$  cross section. The  $M_W$  values, measured in the space-like region, are in good agreement with and complementary to the time-like measurements from LEP and Tevatron.

## 6. NLO QCD analysis of data on DIS

The global NLO QCD fit to ZEUS data [5], including measurements until 1997, and to fixed target data from BCDMS, NMC, E665 and CCFR uses the full information on point-to-point correlations of systematic uncertainties. The data used cover the kinematic range  $2.5 < Q^2 < 30\,000$  GeV<sup>2</sup> and  $6.3 \times 10^{-5} < x < 0.65$ . The fit, displayed in Fig. 6, gives an excellent description of the data down to  $Q^2 \approx 0.8$  GeV<sup>2</sup>.

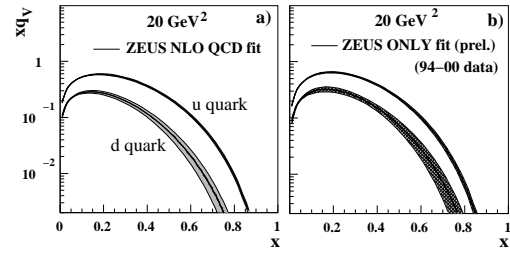


Figure 7. Valence quark distributions from a) the standard ZEUS fit and b) the fit to ZEUS data only, including the 1998–2000 data.

The new precise ZEUS data yield information on the gluon distribution and the quark density at low  $x$ . A fit to the data with  $\alpha_s$  free gives  $\alpha_s = 0.1166 \pm 0.0053$ . The uncertainty of the PDFs is dominated by the correlated systematics. The ZEUS fit is compatible with both the MRST2001 and CTEQ6M parameterizations.

A fit to ZEUS only data including the newest data from 1998–2000, displayed in Fig. 7 b) yields similar uncertainties on the valence quark PDFs as the standard fit, shown in Fig. 7 a), which includes the fixed target data.

## 7. Summary

Recent precision DIS data from ZEUS complete the coverage of a large area of the kinematic plane spanning 6 orders of magnitude in  $x$  and  $Q^2$ . All ZEUS results are fitted consistently by NLO QCD and yield precise PDFs.

## REFERENCES

1. ZEUS Coll., Abstract 850, 31<sup>st</sup> International Conference on High Energy Physics, Amsterdam, Netherlands, 2002.
2. ZEUS Coll., Abstract 771, 31<sup>st</sup> International Conference on High Energy Physics, Amsterdam, Netherlands, 2002.
3. ZEUS Coll., S. Chekanov et al., Preprint DESY-02-113, 2002, ICHEP abstract 766.
4. ZEUS Coll., S. Chekanov et al., Phys. Lett. **B 539**, 197 (2002), ICHEP abstract 763.
5. ZEUS Coll., S. Chekanov et al., Preprint DESY-02-105, 2002, ICHEP abstract 765.